Static and vibration analysis of functionally graded beams using refined shear deformation theory

Thuc P. Vo[a,*], Huu-Tai Thai[b], Trung-Kien Nguyen[c], Fawad Inam[d]

[a]*School of Engineering, Glyndŵr University, Mold Road, Wrexham LL11 2AW, UK.*
[b]*Department of Civil and Environmental Engineering, Hanyang University, 17 Haengdang-dong, Seongdong-gu, Seoul 133-791, Republic of Korea.*
[c]*Faculty of Civil Engineering and Applied Mechanics, University of Technical Education Ho Chi Minh City, 1 Vo Van Ngan Street, Thu Duc District, Ho Chi Minh City, Vietnam*
[d]*Faculty of Engineering and Environment, Northumbria University, Newcastle upon Tyne, NE1 8ST, UK.*

Abstract

Static and vibration analysis of functionally graded beams using refined shear deformation theory is presented. The developed theory, which does not require shear correction factor, accounts for shear deformation effect and coupling coming from the material anisotropy. Governing equations of motion are derived from the Hamilton's principle. The resulting coupling is referred to as triply coupled axial-flexural response. **A two-noded Hermite-cubic element with five degree-of-freedom per node is developed to solve the problem. Numerical results are obtained for functionally graded beams with simply-supported, cantilever-free and clamped-clamped boundary conditions to investigate effects of the power-law exponent and modulus ratio on the displacements, natural frequencies and corresponding mode shapes**.

Keywords: Functionally graded beams; refined shear deformation theory; triply coupled response; finite element model

1. Introduction

Functionally graded (FG) materials are a class of composites that have continuous variation of material properties from one surface to another and thus eliminate the stress concentration found in laminated composites. Typically, FG material is made from a mixture of a ceramic and a metal in such a way that the ceramic can resist high temperature in thermal environments, whereas the metal can decrease the tensile stress occurring on the ceramic surface at the earlier state of cooling. Understanding static and dynamic behaviour of FG beams is of increasing importance. Many theoretical

*Corresponding author, tel.: +44 1978 293979
Email address: t.vo@glyndwr.ac.uk (Thuc P. Vo)

models and beam theories have been developed to solve this complicated problem. By using a meshless local Petrov-Galerkin method, Ching and Yen [1] presented numerical solutions for two-dimensional (2D) FG solids such as simply-supported beams. In terms of Airy stress function, Zhong and Yu [2] presented a general 2D solution for a cantilever FG beam with arbitrary variations of material properties. Birsan et al. [3] employed the theory of directed curves to investigate the mechanical behaviour of non-homogeneous, composite, and FG beams. Based on the classical beam theory (CBT), Sankar and Zhu ([4], [5]) gave an elasticity solution for FG beams under static transverse loads. **Simsek and Kocaturk [6] investigated free vibration characteristics and the dynamic behavior of simply-supported FG beam under a concentrated moving harmonic load. Khalili et al. [7] combined the Rayleigh-Ritz method and the differential quadrature method to solve forced vibration analysis of FG beams subjected to moving loads**. Alshorbagy et al. [8] presented the dynamic characteristics of FG beams with material graduation in axially or transversally through the thickness. It is well known that the CBT is more suitable for slender beams and lower modes of vibration, and becomes inadequate to characterize higher modes of vibration, in particular for short beams. Thus, the first-order beam theory (FOBT) is proposed to overcome the limitations of the CBT by accounting for the transverse shear effects. Based on this theory, Chakraborty et al. [9] proposed a new beam finite element to study static, free vibration and wave propagation problems of FG beams. Li [10] presented a new unified approach for analyzing the static and dynamic behaviours of FG beams with the rotary inertia and shear deformation included. Sina et al. [11] derived analytical solution for free vibration of FG beams. Since the FOBT violates the zero shear stress conditions on the top and bottom surfaces of the beam, a shear correction factor is required to account for the discrepancy between the actual stress state and the assumed constant stress state. To remove the discrepancies in the CBT and FOBT, the higher-order beam theory (HOBT) is developed to avoid the use of shear correction factor and has a better prediction of response of FG beams. The HOBT can be formulated based on the assumption of the higher-order variation of axial displacement or both axial and transverse displacements through the beam depth. **Although there are many references available on static ([12]-[17]) and vibration ([18]-[23]), the research on the displacements and natural frequencies of FG beams in a unitary manner is limited**. Kapuria et al. [24] presented a finite element model for static and free vibration responses of layered FG beams using third-order zigzag theory and validated against experiments. Thai and Vo [25] used the Navier procedure to determine the analytical solution of a simply-supported FG beam by using various higher-order shear deformation beam theories. **To the best of the authors' knowledge, there is no publication available that uses finite element model to deal with displacements,**

higher modes of vibration and corresponding mode shapes of FG beams with various boundary conditions using refined shear deformation theory in the open literature. This complicated problem is not well-investigated and there is a need for further studies.

In this paper, static and vibration analysis of FG beams using refined shear deformation theory is presented. The developed theory, which does not require shear correction factor, accounts for shear deformation effect and coupling coming from the material anisotropy. Governing equations of motion are derived from the Hamilton's principle. The resulting coupling is referred to as triply coupled axial-flexural response. **A two-noded Hermite-cubic element with five degree-of-freedom per node is developed to solve the problem. Numerical results are obtained for FG beams with simply-supported, cantilever-free and clamped-clamped boundary conditions to investigate effects of the power-law exponent and modulus ratio on the displacements, natural frequencies and corresponding mode shapes**.

2. Kinematics

Consider a FG beam with length L and rectangular cross-section $b \times h$, with b being the width and h being the height. The x-, y-, and z-axes are taken along the length, width, and height of the beam, respectively, as shown in Fig. 1. To derive the finite element model of a FG beam, the following assumptions are made for the displacement field:

(a) The axial and transverse displacements consist of bending and shear components in which the bending components do not contribute toward shear forces and, likewise, the shear components do not contribute toward bending moments.

(b) The bending component of axial displacement is similar to that given by the Euler-Bernoulli beam theory.

(c) The shear component of axial displacement gives rise to the higher-order variation of shear strain and hence to shear stress through the beam depth in such a way that shear stress vanishes on the top and bottom surfaces.

The displacement field of the present theory, based on Reddy [26], can be obtained as:

$$U(x,z,t) = u(x,t) - z\frac{\partial w_b(x,t)}{\partial x} - \frac{4z^3}{3h^2}\frac{\partial w_s(x,t)}{\partial x} \tag{1a}$$

$$W(x,z,t) = w_b(x,t) + w_s(x,t) \tag{1b}$$

where u is the axial displacement, w_b and w_s are the bending and shear components of transverse displacement along the mid-plane of the beam.

The non-zero strains are given by:

$$\epsilon_x = \frac{\partial U}{\partial x} = \epsilon_x^\circ + z\kappa_x^b + f(z)\kappa_x^s \tag{2a}$$

$$\gamma_{xz} = \frac{\partial W}{\partial x} + \frac{\partial U}{\partial z} = \big[1 - f'(z)\big]\gamma_{xz}^\circ = g(z)\gamma_{xz}^\circ \tag{2b}$$

where

$$f = \frac{4z^3}{3h^2} \tag{3a}$$

$$g = 1 - f' = 1 - \frac{4z^2}{h^2} \tag{3b}$$

and $\epsilon_x^\circ, \gamma_{xz}^\circ, \kappa_x^b$ and κ_x^s are the axial strain, shear strain and curvatures in the beam, respectively, defined as:

$$\epsilon_x^\circ = u' \tag{4a}$$

$$\gamma_{xz}^\circ = w_s' \tag{4b}$$

$$\kappa_x^b = -w_b'' \tag{4c}$$

$$\kappa_x^s = -w_s'' \tag{4d}$$

where differentiation with respect to the x-axis is denoted by primes ($'$).

3. Variational Formulation

In order to derive the equations of motion, Hamilton's principle is used:

$$\delta \int_{t_1}^{t_2} (\mathcal{K} - \mathcal{U} - \mathcal{V}) dt = 0 \tag{5}$$

where $\mathcal{U}, \mathcal{V}$ and $\mathcal{K}$ denote the strain energy, work done by external forces, and kinetic energy, respectively.

The variation of the strain energy can be stated as:

$$\delta\mathcal{U} = \int_v (\sigma_x \delta\epsilon_x + \sigma_{xz}\delta\gamma_{xz}) dv = \int_0^l (N_x \delta\epsilon_z^\circ + M_x^b \delta\kappa_x^b + M_x^s \delta\kappa_x^s + Q_{xz}\delta\gamma_{xz}^\circ) dx \tag{6}$$

where N_x, M_x^b, M_x^s and Q_{xz} are the axial force, bending moments and shear force, respectively, defined by integrating over the cross-sectional area A as:

$$N_x = \int_A \sigma_x dA \tag{7a}$$

$$M_x^b = \int_A \sigma_x z dA \tag{7b}$$

$$M_x^s = \int_A \sigma_x f(z) dA \tag{7c}$$

$$Q_{xz} = \int_A \sigma_{xz} g(z) dA \tag{7d}$$

The variation of work done by external forces can be written as:

$$\delta\mathcal{V} = -\int_0^l \left[\mathcal{P}_x \delta u + \mathcal{P}_z(\delta w_b + \delta w_s)\right] dx \tag{8}$$

The variation of the kinetic energy is obtained as:

$$\begin{aligned}
\delta\mathcal{K} &= \int_v \rho(z)(\dot{U}\delta\dot{U} + \dot{W}\delta\dot{W}) dv \\
&= \int_0^l \Big[\delta\dot{u}(m_0\dot{u} - m_1\dot{w_b}' - m_f\dot{w_s}') + \delta\dot{w_b} m_0(\dot{w_b} + \dot{w_s}) + \delta\dot{w_b}'(-m_1\dot{u} + m_2\dot{w_b}' + m_{fz}\dot{w_s}') \\
&+ \delta\dot{w_s} m_0(\dot{w_b} + \dot{w_s}) + \delta\dot{w_s}'(-m_f\dot{u} + m_{fz}\dot{w_b}' + m_{f^2}\dot{w_s}')\Big] dx
\end{aligned} \tag{9}$$

where the differentiation with respect to the time t is denoted by dot-superscript convention; $\rho(z)$ is the mass density and $m_0, m_1, m_2, m_f, m_{fz}$ and m_{f^2} are the inertia coefficients, defined by:

$$m_f = \int_A f(z)\rho(z) dA = \frac{4m_3}{3h^2} \tag{10a}$$

$$m_{fz} = \int_A z f(z)\rho(z) dA = \frac{4m_4}{3h^2} \tag{10b}$$

$$m_{f^2} = \int_A f^2(z)\rho(z) dA = \frac{16m_6}{9h^4} \tag{10c}$$

where:

$$(m_0, m_1, m_2, m_3, m_4, m_6) = \int_A \rho(z)(1, z, z^2, z^3, z^4, z^6) dA \tag{11}$$

By substituting Eqs. (6), (8) and (9) into Eq. (5), the following weak statement is obtained:

$$\begin{aligned}
0 &= \int_{t_1}^{t_2}\int_0^l \Big[\delta\dot{u}(m_0\dot{u} - m_1\dot{w_b}' - m_f\dot{w_s}') + \delta\dot{w_b} m_0(\dot{w_b} + \dot{w_s}) + \delta\dot{w_b}'(-m_1\dot{u} + m_2\dot{w_b}' + m_{fz}\dot{w_s}') \\
&+ \delta\dot{w_s} m_0(\dot{w_b} + \dot{w_s}) + \delta\dot{w_s}'(-m_f\dot{u} + m_{fz}\dot{w_b}' + m_{f^2}\dot{w_s}') \\
&- \mathcal{P}_x\delta u - \mathcal{P}_z(\delta w_b + \delta w_s) - N_x\delta u' + M_x^b\delta w_b'' + M_x^s\delta w_s'' - Q_{xz}\delta w_s'\Big] dx dt
\end{aligned} \tag{12}$$

4. Constitutive Equations

The material properties of FG beams are assumed to vary continuously through the beam depth by a power-law as [27]:

$$P(z) = (P_u - P_l)(\frac{1}{2} + \frac{z}{h})^n + P_l \tag{13}$$

where P represents the effective material property such as Young's modulus E, Poisson's ratio ν, and mass density ρ; subscripts u and l represent the upper and lower surface constituents, respectively; and n is the power-law exponent. It is clear that when $z = -h/2$, $P = P_l$ and when $z = h/2$, $P = P_u$. The stress-strain relations for FG beams are given by:

$$\sigma_x = E(z)\gamma_x \tag{14a}$$

$$\sigma_{xz} = \frac{E(z)}{2\big[1+\nu(z)\big]}\gamma_{xz} = G(z)\gamma_{xz} \tag{14b}$$

The constitutive equations for bar forces and bar strains are obtained by using Eqs. (2), (7) and (14):

$$\begin{Bmatrix} N_x \\ M_x^b \\ M_x^s \\ Q_{xz} \end{Bmatrix} = \begin{bmatrix} R_{11} & R_{12} & R_{13} & 0 \\ & R_{22} & R_{23} & 0 \\ & & R_{33} & 0 \\ \text{sym.} & & & R_{44} \end{bmatrix} \begin{Bmatrix} \epsilon_x^\circ \\ \kappa_x^b \\ \kappa_x^s \\ \gamma_{xz}^\circ \end{Bmatrix} \tag{15}$$

where R_{ij} are the stiffnesses of FG beams and given by:

$$R_{11} = \int_z E(z)bdz \tag{16a}$$

$$R_{12} = \int_z zE(z)bdz \tag{16b}$$

$$R_{13} = \int_z f(z)E(z)bdz \tag{16c}$$

$$R_{22} = \int_z z^2E(z)bdz \tag{16d}$$

$$R_{23} = \int_z zf(z)E(z)bdz \tag{16e}$$

$$R_{33} = \int_z f^2(z)E(z)bdz \tag{16f}$$

$$R_{44} = \int_z g^2(z)G(z)bdz \tag{16g}$$

5. Governing equations of motion

The equilibrium equations of the present study can be obtained by integrating the derivatives of the varied quantities by parts and collecting the coefficients of $\delta u, \delta w_b$ and δw_s:

$$N_x' + \mathcal{P}_x = m_0\ddot{u} - m_1\ddot{w}_b{}' - m_f\ddot{w}_s{}' \tag{17a}$$

$$M_x^{b\prime\prime} + \mathcal{P}_z = m_0(\ddot{w}_b + \ddot{w}_s) + m_1\ddot{u}' - m_2\ddot{w}_b{}'' - m_{fz}\ddot{w}_s{}'' \tag{17b}$$

$$M_x^{s\prime\prime} + Q_{xz}' + \mathcal{P}_z = m_0(\ddot{w}_b + \ddot{w}_s) + m_f\ddot{u}' - m_{fz}\ddot{w}_b{}'' - m_{f^2}\ddot{w}_s{}'' \tag{17c}$$

The natural boundary conditions are of the form:

$$\delta u \;:\; N_x \tag{18a}$$

$$\delta w_b \;:\; M_x^{b\prime} - m_1\ddot{u} + m_2\ddot{w}_b{}' + m_{fz}\ddot{w}_s{}' \tag{18b}$$

$$\delta w_b' \;:\; M_x^b \tag{18c}$$

$$\delta w_s \;:\; M_x^{s\prime} + Q_{xz} - m_f\ddot{u} + m_{fz}\ddot{w}_b{}' + m_{f^2}\ddot{w}_s{}' \tag{18d}$$

$$\delta w_s' \;:\; M_x^s \tag{18e}$$

By substituting Eqs. (4) and (15) into Eq. (17), the explicit form of the governing equations of motion can be expressed with respect to the stiffnesses R_{ij}:

$$R_{11}u'' - R_{12}w_b''' - R_{13}w_s''' + \mathcal{P}_x = m_0\ddot{u} - m_1\ddot{w}_b{}' - m_f\ddot{w}_s{}' \tag{19a}$$

$$\begin{aligned} R_{12}u''' - R_{22}w_b^{iv} - R_{23}w_s^{iv} + \mathcal{P}_z &= m_0(\ddot{w}_b + \ddot{w}_s) + m_1\ddot{u}' \\ &- m_2\ddot{w}_b{}'' - m_{fz}\ddot{w}_s{}'' \end{aligned} \tag{19b}$$

$$\begin{aligned} R_{13}u''' - R_{23}w_b^{iv} - R_{33}w_s^{iv} + R_{44}w_s'' + \mathcal{P}_z &= m_0(\ddot{w}_b + \ddot{w}_s) + m_f\ddot{u}' \\ &- m_{fz}\ddot{w}_b{}'' - m_{f^2}\ddot{w}_s{}'' \end{aligned} \tag{19c}$$

Eq. (19) is the most general form for the static and vibration analysis of FG beams, and the dependent variables, u, w_b and w_s are fully coupled. The resulting coupling is referred to as triply axial-flexural coupled response.

6. Finite Element Formulation

The present theory for FG beams described in the previous section was implemented via a displacement based finite element method. The variational statement in Eq. (12) requires that the bending and shear components of transverse displacement w_b and w_s be twice differentiable and C^1-continuous, whereas the axial displacement u must be only once differentiable and C^0-continuous. The generalized displacements are expressed over each element as a combination of the linear interpolation function Ψ_j for u and Hermite-cubic interpolation function ψ_j for w_b and w_s associated with node j and the nodal values:

$$u = \sum_{j=1}^{2} u_j\Psi_j \tag{20a}$$

$$w_b = \sum_{j=1}^{4} w_{bj}\psi_j \tag{20b}$$

$$w_s = \sum_{j=1}^{4} w_{sj}\psi_j \tag{20c}$$

For static problem, by omitting the inertia terms and substituting expressions in Eq. (20) into the weak statement in Eq. (12), the finite element model of a typical element can be expressed as:

$$[K]\{\Delta\} = \{F\} \tag{21}$$

where $\{\Delta\}$ is the nodal displacements and $[K]$, $[F]$ is the element stiffness matrix, the element force vector, given by:

$$K_{ij}^{11} = \int_0^l R_{11}\Psi_i'\Psi_j' dx \tag{22a}$$

$$K_{ij}^{12} = -\int_0^l R_{12}\Psi_i'\psi_j'' dx \tag{22b}$$

$$K_{ij}^{13} = -\int_0^l R_{13}\Psi_i'\psi_j'' dx \tag{22c}$$

$$K_{ij}^{22} = \int_0^l R_{22}\psi_i''\psi_j'' dx \tag{22d}$$

$$K_{ij}^{23} = \int_0^l R_{23}\psi_i''\psi_j'' dx \tag{22e}$$

$$K_{ij}^{33} = \int_0^l (R_{33}\psi_i''\psi_j'' + R_{44}\psi_i'\psi_j') dx \tag{22f}$$

$$F_i^1 = \int_0^l \mathcal{P}_x\Psi_i dz \tag{22g}$$

$$F_i^2 = \int_0^l \mathcal{P}_z\psi_i dx \tag{22h}$$

$$F_i^3 = \int_0^l \mathcal{P}_z\psi_i dx \tag{22i}$$

For vibration problem, the dynamic equation can be expressed as the following eigenvalue problem:

$$([K] - \omega^2[M])\{\Delta\} = \{0\} \tag{23}$$

where $\{\Delta\}$ is the eigenvector of nodal displacements and $[M]$ is the element mass matrix, given by:

$$M_{ij}^{11} = \int_0^l m_0\Psi_i\Psi_j dx \tag{24a}$$

$$M_{ij}^{12} = -\int_0^l m_1\Psi_i\psi_j' dx \tag{24b}$$

$$M_{ij}^{13} = -\int_0^l m_f\Psi_i\psi_j' dx \tag{24c}$$

$$M_{ij}^{22} = \int_0^l (m_0\psi_i\psi_j + m_2\psi_i'\psi_j')dx \tag{24d}$$

$$M_{ij}^{23} = \int_0^l (m_0\psi_i\psi_j + m_{fz}\psi_i'\psi_j')dx \tag{24e}$$

$$M_{ij}^{33} = \int_0^l (m_0\psi_i\psi_j + m_{f2}\psi_i'\psi_j')dx \tag{24f}$$

7. Numerical Examples

In this section, a number of numerical examples are analysed for verification the accuracy of present study and investigation the displacements, natural frequencies and corresponding mode shapes of FG beams. In the case of the FOBT, a value of $K_s = 5/6$ is used for the shear correction factor. For convenience, the following non-dimensional terms are used, the axial and vertical displacement of FG beams under the uniformly distributed load q:

$$\overline{u} = \frac{u}{K}\frac{E_{Al}I}{qL^4} \tag{25a}$$

$$\overline{w} = \frac{w}{K}\frac{E_{Al}I}{qL^4} \tag{25b}$$

and the natural frequencies:

$$\overline{\omega} = \frac{\omega L^2}{h}\sqrt{\frac{\rho_{Al}}{E_{Al}}} \tag{26}$$

as well as Young's modulus ratio:

$$E_{\text{ratio}} = \frac{E_u}{E_l} \tag{27a}$$

where $I = \dfrac{bh^3}{12}$ and $K = \dfrac{5}{384}, \dfrac{1}{8}$ and $\dfrac{1}{384}$ for simply-supported, cantilever-free and clamped-clamped boundary conditions, respectively.

7.1. Results for static analysis

For verification purpose, simply-supported FG beams with two span-to-height ratios $L/h = 4$ and 16 under a uniform load q are considered first. FG material properties obtained from [15] are composed of Aluminum in the upper surface (Al: $E_u = E_{Al} = 70\text{GPa}, \nu_{Al} = 0.3$) and Zirconia in the lower surface (ZnO_2: $E_l = 200\text{GPa}, \nu_l = 0.3$). It should be noted that as the power-law exponent increases, the FG beam approaches to the full ceramic one and Young's modulus ratio (E_{ratio}) is smaller than unity. The mid-span displacements for various values of power-law exponent are compared with previous results ([15], [25]) in Table 1. The analytical solutions using HOBT were given in Thai and Vo [25]

and derived here for comparison. The results obtained from the FOBT and HOBT are very close to each other. It can be seen that the current solutions are in excellent agreement with previous studies. It seems that for the FOBT, Simsek [15] uses the shear correction factor $K_s = 1.0$. The bending and shear components of vertical displacement and axial displacement along the length of the beam are plotted in Figs. 2 and 3. All the displacements decrease with increasing value of the power-law exponent. This is due to the fact that the higher power-law exponent causes axial-flexural coupling effect, which results in an increase in axial and flexural stiffness. It is from Fig. 3 that highlights the effect of this coupling on the axial displacement of beam. This response is never seen in the homogeneous beams (ceramic and metal) because the coupling terms are not present. It also implies that the structure under transverse load not only causes vertical displacement as would be observed, but also causes additional response due solely to coupling effect.

In order to investigate the effects of the power-law exponent on the displacement further, by using HOBT, FG beams with different boundary conditions are considered. Unless mentioned otherwise, the lower surface of FG beams is always assumed to be Aluminum in the following examples. In contrast to previous example, in this case $E_{\text{ratio}} > 1$, all maximum displacements increase as the power-law exponent increases (Table 2). As expected, the highest displacements are obtained for full ceramic beam ($n = 0$) while the lowest ones are obtained for full metal beam ($n = \infty$). The mid-span displacements of simply-supported FG beams are presented in Table 3 and Fig. 4 to show effect of the Young's modulus ratio. It can be seen that for a constant power-law exponent, the displacement decreases with increasing E_{ratio}. Vice versa, for a given value of E_{ratio}, as the power-law exponent increases, it causes contrary responses on the displacement, which is decreased when $E_{\text{ratio}} < 1$ and increased when $E_{\text{ratio}} > 1$ as well as has no change when $E_{\text{ratio}} = 1$ (Fig. 4). It also confirms again some static responses mentioned in the previous examples (Tables 1 and 2).

7.2. Results for vibration analysis

To demonstrate the accuracy and validity of this study further, vibration analysis of FG beams with $L/h = 5$ and 20 is performed. FG material properties are assumed to be [19]: Aluminum in the lower surface (Al: $E_l = E_{Al} = 70\text{GPa}, \nu_{Al} = 0.3, \rho_l = \rho_{Al} = 2702\text{kg/m}^3$) and Alumina in the upper surface (Al_2O_3: $E_u = 380\text{GPa}, \nu_u = 0.3, \rho_u = 3960\text{kg/m}^3$). The fundamental natural frequencies for different boundary conditions are compared with previous results ([19], [25]) in Tables 4 and 5. Again, it can be seen that the FOBT and HOBT give almost the same results. As expected, an increase of the power-law exponent results in a decrease of elasticity modulus and bending rigidity, which leads to a reduction in natural frequency. This reduction is the same for the three boundary conditions. Through the close correlation observed between the present model and the earlier works, accuracy

of the present model is again established. By using HOBT, clamped-clamped FG beams are chosen to investigate the effect of the power-law exponent on the higher vibration modes (Table 6 and Fig. 5). The first four vibration mode shapes corresponding to the power-law exponents $n = 0$ and 5 are illustrated in Fig. 6. It can be seen that for the homogeneous beam, the first, second and fourth modes exhibit double coupled vibration (bending and shear components), whereas, the third mode exhibits axial vibration. However, for the FG beam, all four modes display triply coupled vibration (axial, bending and shear components). This fact explains that triply axial-flexural coupled response should be considered simultaneously for static and vibration analysis of the FG beam.

Finally, effect of Young's modulus ratio on the fundamental natural frequencies of clamped-clamped FG beams is shown in Table 6 and Fig. 7. It can be seen that the natural frequencies increase monotonically with the increase of E_{ratio} for all values power-law exponent considered. This ratio is more pronounced for small values of power-law exponent than large ones (Table 6). For instant, for homogeneous beam with $L/h = 5$ ($n = 0$), the ratio between the fundamental natural frequency corresponding to Young's modulus ratios 0.25 and 6 is 4.9 and similar value for FG beam ($n = 10$) is 1.3. When comparing E_{ratio} with unity, similar response of static behaviour can be observed again for vibration analysis. That is, with the increase in power-law exponent, the natural frequency increases when $E_{\text{ratio}} < 1$, and decreases when $E_{\text{ratio}} > 1$. As expected, when the beam is homogeneous, $E_{\text{ratio}} = 1$, the natural frequency is independent of the power-law exponent (Fig. 7).

8. Conclusions

Finite element model which accounts for shear deformation effect and coupling coming from the material anisotropy is developed to study the static and vibration analysis of FG beams with various boundary conditions. This model is capable of predicting accurately static responses, natural frequencies and corresponding mode shapes. It accounts for parabolical variation of shear strain through the beam depth, and satisfies the zero traction boundary conditions on the top and bottom surfaces of the beam without using shear correction factor. Triply coupled axial-flexural response should be considered simultaneously for accurate analysis of FG beams. The present model is found to be appropriate and efficient in analysing static and vibration problem of FG beams.

Acknowledgements

The third author gratefully acknowledges financial support from Vietnam National Foundation for Science and Technology Development (NAFOSTED) under grant number 107.02-2012.07, and from University of Technical Education Ho Chi Minh City.

References

[1] H. K. Ching, S. C. Yen, Meshless local Petrov-Galerkin analysis for 2D functionally graded elastic solids under mechanical and thermal loads, Composites Part B: Engineering 36 (3) (2005) 223 – 240.

[2] Z. Zhong, T. Yu, Analytical solution of a cantilever functionally graded beam, Composites Science and Technology 67 (3-4) (2007) 481 – 488.

[3] M. Birsan, H. Altenbach, T. Sadowski, V. Eremeyev, D. Pietras, Deformation analysis of functionally graded beams by the direct approach, Composites Part B: Engineering 43 (3) (2012) 1315 – 1328.

[4] B. V. Sankar, An elasticity solution for functionally graded beams, Composites Science and Technology 61 (5) (2001) 689 – 696.

[5] H. Zhu, B. V. Sankar, A Combined Fourier Series–Galerkin Method for the Analysis of Functionally Graded Beams, Journal of Applied Mechanics 71 (3) (2004) 421–424.

[6] M. Simsek, T. Kocaturk, Free and forced vibration of a functionally graded beam subjected to a concentrated moving harmonic load, Composite Structures 90 (4) (2009) 465 – 473.

[7] S. M. R. Khalili, A. A. Jafari, S. A. Eftekhari, A mixed Ritz-DQ method for forced vibration of functionally graded beams carrying moving loads, Composite Structures 92 (10) (2010) 2497 – 2511.

[8] A. E. Alshorbagy, M. Eltaher, F. Mahmoud, Free vibration characteristics of a functionally graded beam by finite element method, Applied Mathematical Modelling 35 (1) (2011) 412 – 425.

[9] A. Chakraborty, S. Gopalakrishnan, J. N. Reddy, A new beam finite element for the analysis of functionally graded materials, International Journal of Mechanical Sciences 45 (3) (2003) 519 – 539.

[10] X.-F. Li, A unified approach for analyzing static and dynamic behaviors of functionally graded Timoshenko and Euler-Bernoulli beams, Journal of Sound and Vibration 318 (4-5) (2008) 1210 – 1229.

[11] S. A. Sina, H. M. Navazi, H. Haddadpour, An analytical method for free vibration analysis of functionally graded beams, Materials & Design 30 (3) (2009) 741 – 747.

[12] R. Kadoli, K. Akhtar, N. Ganesan, Static analysis of functionally graded beams using higher order shear deformation theory, Applied Mathematical Modelling 32 (12) (2008) 2509 – 2525.

[13] M. Benatta, I. Mechab, A. Tounsi, E. A. Bedia, Static analysis of functionally graded short beams including warping and shear deformation effects, Computational Materials Science 44 (2) (2008) 765 – 773.

[14] S. Ben-Oumrane, T. Abedlouahed, M. Ismail, B. B. Mohamed, M. Mustapha, A. B. E. Abbas, A theoretical analysis of flexional bending of Al/Al2O3 S-FGM thick beams, Computational Materials Science 44 (4) (2009) 1344 – 1350.

[15] M. Simsek, Static analysis of a functionally graded beam under a uniformly distributed load by Ritz method, International Journal of Engineering and Applied Sciences 1 (3) (2009) 1–11.

[16] G. Giunta, S. Belouettar, E. Carrera, Analysis of FGM Beams by Means of Classical and Advanced Theories, Mechanics of Advanced Materials and Structures 17 (8) (2010) 622–635.

[17] X.-F. Li, B.-L. Wang, J.-C. Han, A higher-order theory for static and dynamic analyses of functionally graded beams, Archive of Applied Mechanics 80 (2010) 1197–1212.

[18] M. Aydogdu, V. Taskin, Free vibration analysis of functionally graded beams with simply supported edges, Materials & Design 28 (5) (2007) 1651 – 1656.

[19] M. Simsek, Fundamental frequency analysis of functionally graded beams by using different higher-order beam theories, Nuclear Engineering and Design 240 (4) (2010) 697 – 705.

[20] M. Simsek, Vibration analysis of a functionally graded beam under a moving mass by using different beam theories, Composite Structures 92 (4) (2010) 904 – 917.

[21] G. Giunta, D. Crisafulli, S. Belouettar, E. Carrera, Hierarchical theories for the free vibration analysis of functionally graded beams, Composite Structures 94 (1) (2011) 68 – 74.

[22] M. Salamat-talab, A. Nateghi, J. Torabi, Static and dynamic analysis of third-order shear deformation FG micro beam based on modified couple stress theory, International Journal of Mechanical Sciences 57 (1) (2012) 63 – 73.

[23] A. Nateghi, M. Salamat-talab, J. Rezapour, B. Daneshian, Size dependent buckling analysis of functionally graded micro beams based on modified couple stress theory, Applied Mathematical Modelling 36 (10) (2012) 4971 – 4987.

[24] S. Kapuria, M. Bhattacharyya, A. N. Kumar, Bending and free vibration response of layered functionally graded beams: A theoretical model and its experimental validation, Composite Structures 82 (3) (2008) 390 – 402.

[25] H.-T. Thai, T. P. Vo, Bending and free vibration of functionally graded beams using various higher-order shear deformation beam theories, International Journal of Mechanical Sciences 62 (1) (2012) 57 – 66.

[26] J. N. Reddy, A simple higher-order theory for laminated composite plates, Journal of Applied Mechanics 51 (4) (1984) 745–752.

[27] J. N. Reddy, Mechanics of laminated composite plates and shells: theory and analysis, CRC, 2004.

CAPTIONS OF TABLES

Table 1: Comparison of non-dimensional mid-span displacements of simply-supported FG beams with various values of power-law exponent under a uniformly distributed load.

Table 2: Non-dimensional maximum displacements of FG beams with various values of power-law exponent for different boundary conditions.

Table 3: Effects of Young's modulus ratio on non-dimensional mid-span displacements of simply-supported FG beams with various values of power-law exponent.

Table 4: Comparison of the non-dimensional fundamental natural frequencies of FG beams with various values of power-law exponent for different boundary conditions (L/h=5).

Table 5: Comparison of the non-dimensional fundamental natural frequencies of FG beams with various values of power-law exponent for different boundary conditions (L/h=20).

Table 6: The first four non-dimensional natural frequencies of clamped-clamped FG beams with various values of power-law exponent.

Table 7: Effects of Young's modulus ratio on non-dimensional fundamental natural frequencies of clamped-clamped FG beams with various values of power-law exponent.

Table 1: Comparison of non-dimensional mid-span displacements of simply-supported FG beams with various values of power-law exponent under a uniformly distributed load.

L/h	Theory	Reference	Power-law exponent n						
			0	0.2	0.5	1	2	5	Full ceramic
4	FOBT	Simsek [13]	1.13002	0.84906	0.71482	0.62936	0.56165	0.49176	0.39550
		Present (K_s=1)	1.13000	0.84859	0.71472	0.62933	0.56163	0.49175	0.39550
		Present (K_s=5/6)	1.15600	0.86845	0.73078	0.64281	0.57325	0.50196	0.40460
	HOBT	Simsek [13]	1.15578	0.87145	0.73264	0.64271	0.57142	0.49978	0.40452
		Thai & Vo [20]	1.15576	0.87100	0.73256	0.64271	0.57141	0.49978	0.40453
		Present	1.15580	0.87098	0.73254	0.64268	0.57140	0.49977	0.40452
16	FOBT	Simsek [13]	1.00812	0.75595	0.63953	0.56615	0.50718	0.44391	0.35284
		Present (K_s=1)	1.00810	0.75552	0.63944	0.56613	0.50717	0.44391	0.35284
		Present (K_s=5/6)	1.00980	0.75676	0.64045	0.56698	0.50790	0.44455	0.35341
	HOBT	Simsek [13]	1.00975	0.75737	0.64065	0.56699	0.50780	0.44442	0.35341
		Thai & Vo [20]	1.00975	0.75695	0.64059	0.56700	0.50781	0.44442	0.35341
		Present	1.00970	0.75694	0.64056	0.56698	0.50779	0.44442	0.35341

Table 2: Non-dimensional maximum displacements of FG beams with various values of power-law exponent for different boundary conditions.

L/h	Theory	Power-law exponent n						
		0	0.2	1	2	5	10	Full metal
4	*Simply- Supported beam*							
	FOBT	0.40460	0.46874	0.64281	0.73516	0.82401	0.89517	1.06500
	HOBT	0.40452	0.46805	0.64269	0.73884	0.83544	0.90566	1.06321
	Cantilever- Free beam							
	FOBT	0.37275	0.43302	0.59564	0.67897	0.75453	0.81732	1.06500
	HOBT	0.37212	0.43209	0.59471	0.67937	0.75773	0.81997	1.06321
	Clamped- Clamped beam							
	FOBT	0.62300	0.71366	0.96628	1.12044	1.30041	1.42898	1.78000
	HOBT	0.60773	0.69410	0.94365	1.11025	1.31813	1.43793	1.73637
16	*Simply- Supported beam*							
	FOBT	0.35341	0.41133	0.56698	0.64483	0.71232	0.77004	1.00406
	HOBT	0.35341	0.41129	0.56698	0.64507	0.71305	0.77071	1.00403
	Cantilever- Free beam							
	FOBT	0.35142	0.40910	0.56404	0.64134	0.70800	0.76518	1.00406
	HOBT	0.35141	0.40907	0.56402	0.64141	0.70827	0.76543	1.00403
	Clamped- Clamped beam							
	FOBT	0.36706	0.42663	0.58711	0.66879	0.74200	0.80335	1.04875
	HOBT	0.36676	0.42611	0.58667	0.66943	0.74488	0.80586	1.04789

Table 3: Effects of Young's modulus ratio on non-dimensional mid-span displacements of simply-supported FG beams with various values of power-law exponent.

L/h	E_{ratio}	Power-law exponent n					
		0	0.2	1	2	5	10
4	0.25	4.62303	3.07753	2.06729	1.77017	1.48969	1.34957
	0.50	2.31152	1.95154	1.59227	1.47372	1.34802	1.27440
	1.00	1.15576	1.15576	1.15576	1.15576	1.15576	1.15576
	2.00	0.57788	0.64422	0.79613	0.86749	0.94125	0.99617
	4.00	0.28894	0.34322	0.51682	0.62979	0.74338	0.82089
	6.00	0.18329	0.22340	0.38874	0.51272	0.64445	0.72504
16	0.25	4.03900	2.67521	1.83367	1.58117	1.32928	1.19678
	0.50	2.01950	1.69790	1.39759	1.30178	1.19301	1.12413
	1.00	1.00975	1.00975	1.00975	1.00975	1.00975	1.00975
	2.00	0.50488	0.56517	0.69879	0.75515	0.80927	0.85675
	4.00	0.25244	0.30197	0.45842	0.55303	0.63163	0.69094
	6.00	0.16829	0.20620	0.34702	0.45453	0.54732	0.60230

Table 4: Comparison of the non-dimensional fundamental natural frequencies of FG beams with various values of power-law exponent for different boundary conditions (L/h=5).

Theory	Reference	Power-law exponent n						
		0	0.2	1	2	5	10	Full metal
Simply-Supported beam								
FOBT	Simsek [17]	5.15247	4.80657	3.99023	3.63438	3.43119	3.31343	2.67718
	Present	5.15260	4.80328	3.97108	3.60495	3.40253	3.29625	2.67725
HOBT	Simsek [17]	5.15274	4.80924	3.99042	3.62643	3.40120	3.28160	2.67732
	Thai &Vo [20]	5.15275	4.80807	3.99042	3.62644	3.40120	3.28160	2.67732
	Present	5.15275	4.80590	3.97160	3.59791	3.37429	3.26534	2.67732
Cantilever-Free beam								
FOBT	Simsek [17]	1.89479	1.76554	1.46300	1.33376	1.26445	1.22398	0.98452
	Present	1.89442	1.76477	1.46279	1.33357	1.26423	1.22372	0.98432
HOBT	Simsek [17]	1.89523	1.76637	1.46328	1.33254	1.25916	1.21834	0.98474
	Present	1.89522	1.76591	1.46333	1.33260	1.25921	1.21837	0.98474
Clamped-Clamped beam								
FOBT	Simsek [17]	10.03440	9.41764	7.92529	7.21134	6.66764	6.34062	5.21382
	Present	9.99836	9.38337	7.90153	7.19013	6.64465	6.31609	5.19506
HOBT	Simsek [17]	10.07050	9.46641	7.95034	7.17674	6.49349	6.16515	5.23254
	Present	10.06780	9.46237	7.95221	7.18011	6.49614	6.16623	5.23113

Table 5: Comparison of the non-dimensional fundamental natural frequencies of FG beams with various values of power-law exponent for different boundary conditions (L/h=20).

Theory	Reference	Power-law exponent n						
		0	0.2	1	2	5	10	Full metal
Simply-Supported beam								
FOBT	Simsek [17]	5.46032	5.08265	4.20505	3.83676	3.65088	3.54156	2.83713
	Present	5.46033	5.08120	4.20387	3.83491	3.64903	3.54045	2.83714
HOBT	Simsek [17]	5.46030	5.08286	4.20503	3.83611	3.64850	3.53896	2.83716
	Thai & Vo [20]	5.46032	5.08152	4.20505	3.83613	3.64849	3.53899	2.83714
	Present	5.46032	5.08139	4.20387	3.83428	3.64663	3.53787	2.83714
Cantilever-Free beam								
FOBT	Simsek [17]	1.94957	1.81456	1.50104	1.36968	1.30375	1.26495	1.01297
	Present	1.94955	1.81408	1.50106	1.36970	1.30376	1.26495	1.01297
HOBT	Simsek [17]	1.94954	1.81458	1.50106	1.36957	1.30332	1.26453	1.01301
	Present	1.94957	1.81412	1.50107	1.36961	1.30337	1.26453	1.01298
Clamped-Clamped beam								
FOBT	Simsek [17]	12.22350	11.38500	9.43135	8.60401	8.16985	7.91275	6.35123
	Present	12.22020	11.37950	9.43114	8.60467	8.16977	7.91154	6.34954
HOBT	Simsek [17]	12.22380	11.38730	9.43158	8.59751	8.14460	7.88576	6.35139
	Present	12.22280	11.38380	9.43282	8.59942	8.14595	7.88616	6.35085

Table 6: The first fournon-dimensional natural frequencies of clamped-clamped FG beams with various values of power-law exponent.

L/h	Theory	Mode	Power-law exponent n						
			0	0.2	1	2	5	10	Full metal
5	FOBT	1	9.99836	9.38337	7.90153	7.19013	6.64465	6.31609	5.19506
		2	23.87540	22.48400	19.04940	17.29240	15.78680	14.90350	12.40540
		3	**30.23910***	28.88370	25.37460	23.01120	19.96340	18.23210	**15.71200***
		4	38.1841	36.0793	30.7500	27.8331	25.0901	23.5501	19.8401
	HOBT	1	10.06780	9.46237	7.95221	7.18011	6.49614	6.16623	5.23113
		2	24.10070	22.74470	19.23920	17.29090	15.34110	14.44980	12.52250
		3	**30.23910***	28.88180	25.35890	22.98670	19.94120	18.22210	**15.71200***
		4	39.0057	36.9454	31.4558	28.1427	24.5432	22.9903	20.2670
20	FOBT	1	12.2202	11.3795	9.43114	8.60467	8.16977	7.91154	6.34954
		2	33.1335	30.8752	25.6223	23.3691	22.1345	21.4015	17.2159
		3	62.9124	58.7017	48.8401	44.5197	41.9748	40.4612	32.6888
		4	101.2440	94.6356	78.8259	71.5625	66.5576	63.9421	52.5615
	HOBT	1	12.2228	11.3838	9.43282	8.59942	8.14595	7.88616	6.35085
		2	33.1428	30.8934	25.6289	23.3419	22.0168	21.2764	17.2207
		3	62.9707	58.7885	48.8815	44.441	41.5861	40.0522	32.719
		4	101.1590	94.4833	78.7578	71.7508	67.4117	64.8394	52.6056

*: Axial natural frequencies; rest ones are flexural natural frequencies

Table 7: Effects of Young's modulus ratio on non-dimensional fundamental natural frequencies of clamped-clamped FG beams with various values of power-law exponent.

L/h	E_{ratio}	Power-law exponent n					
		0	0.2	1	2	5	10
5	0.25	2.61556	3.19340	3.95208	4.29420	4.67863	4.89280
	0.50	3.69897	4.01365	4.47085	4.66897	4.88894	5.01585
	1.00	5.23113	5.23113	5.23113	5.23113	5.23113	5.23113
	2.00	7.39793	7.02721	6.32273	6.02099	5.73085	5.57270
	4.00	10.46230	9.64704	7.90415	7.10516	6.39303	6.04839
	6.00	12.81360	11.69000	9.15438	7.92432	6.85985	6.37865
20	0.25	3.17543	3.90005	4.71863	5.08443	5.54485	5.84075
	0.50	4.49073	4.89588	5.40026	5.59842	5.84901	6.02390
	1.00	6.35085	6.35085	6.35085	6.35085	6.35085	6.35085
	2.00	8.98146	8.49181	7.63712	7.34152	7.08441	6.88553
	4.00	12.70170	11.62020	9.43725	8.58476	8.01053	7.65300
	6.00	15.55640	14.06350	10.85240	9.47646	8.60449	8.18711

CAPTIONS OF FIGURES

Figure 1: Geometry and coordinate of a FG beam

Figure 2: Non-dimensional bending and shear components of vertical displacement along the length of simply-supported FG beam with various values of power-law exponent (L/h=4).

Figure 3: Non-dimensional axial displacement along the length of simply-supported FG beam with various values of power-law exponent (L/h=4).

Figure 4: Effect of Young's modulus ratio on the non-dimensional mid-span displacements of simply-supported FG beam with respect to power-law exponent (L/h=4).

Figure 5: Variation of the first four non-dimensional natural frequencies of a clamped-clamped FG beam with respect to power-law exponent (L/h=5).

Figure 6: Vibration mode shapes of a clamped-clamped FG beam with two values of power-law exponent n=0 and n=5 (L/h=5)

Figure 7: Effect of Young's modulus ratio on the non-dimensional fundamental natural frequencies of clamped-clamped FG beam with respect to power-law exponent (L/h=5).

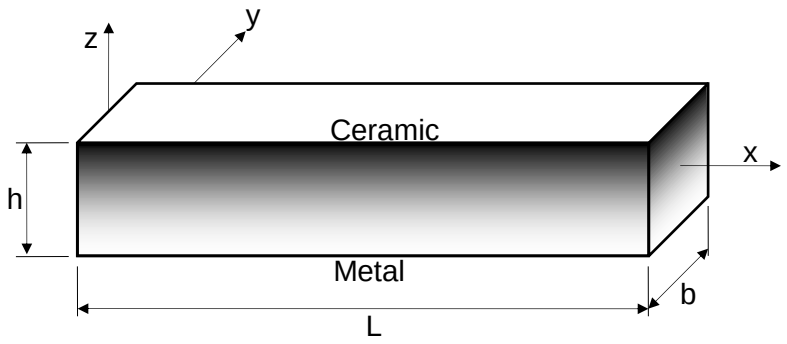

Figure 1: Geometry and coordinate of a FG beam

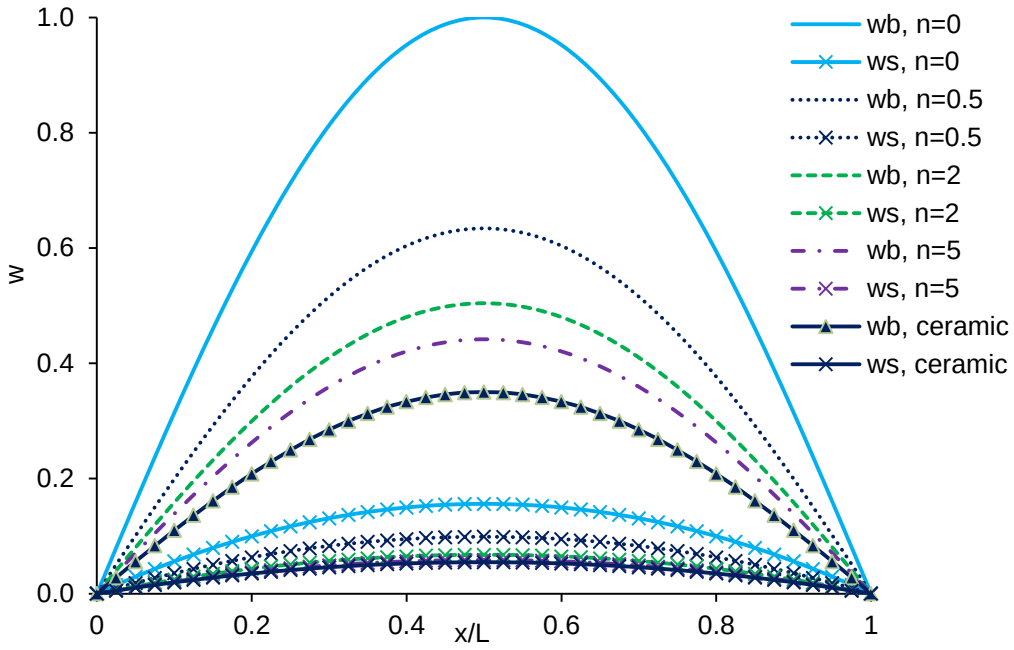

Figure 2: Non-dimensional bending and shear components of vertical displacementalong the length of simply-supported FG beam with various values of power-law exponent(L/h=4).

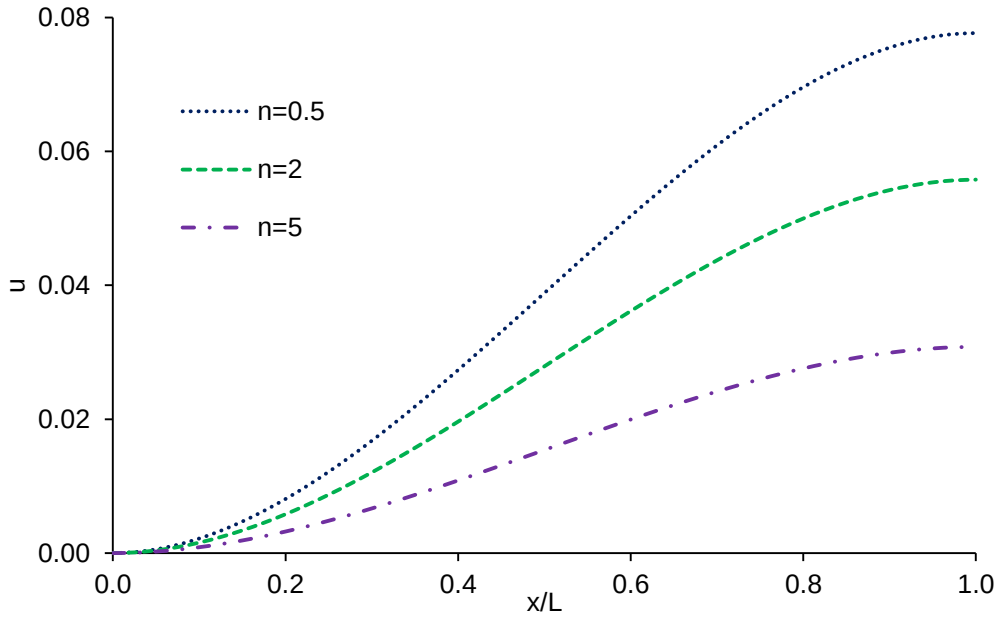

Figure 3: Non-dimensional axial displacement along the length of simply-supported FG beam with various values of power-law exponent(L/h=4).

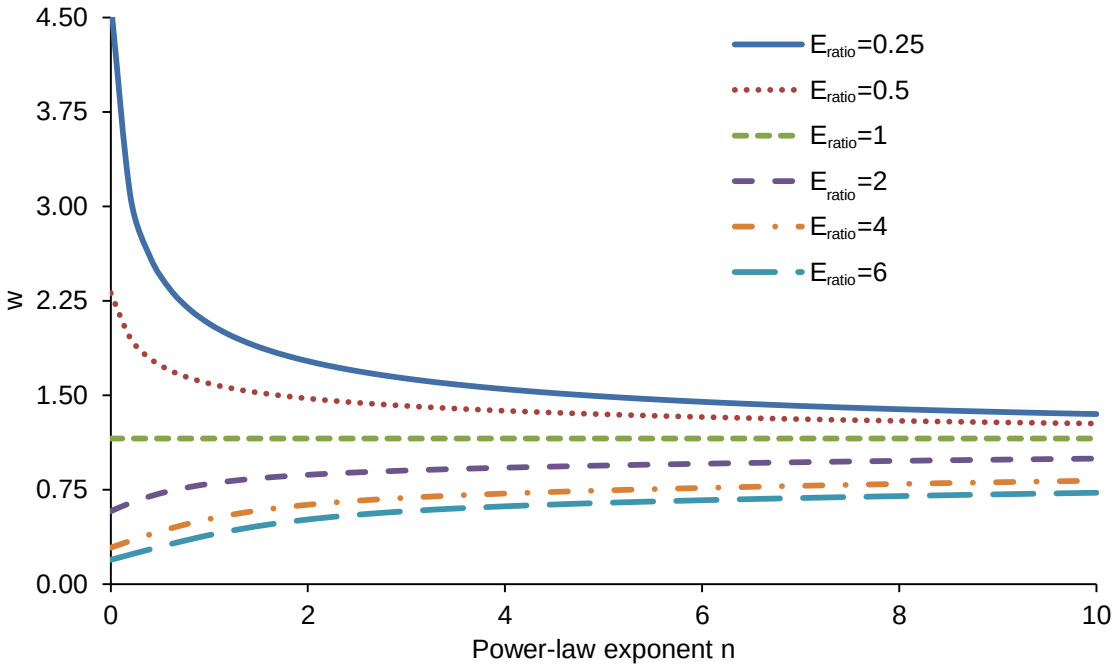

Figure 4: Effect of Young's modulus ratio onthe non-dimensional mid-span displacements of simply-supported FG beamwith respect to power-law exponent (L/h=4).

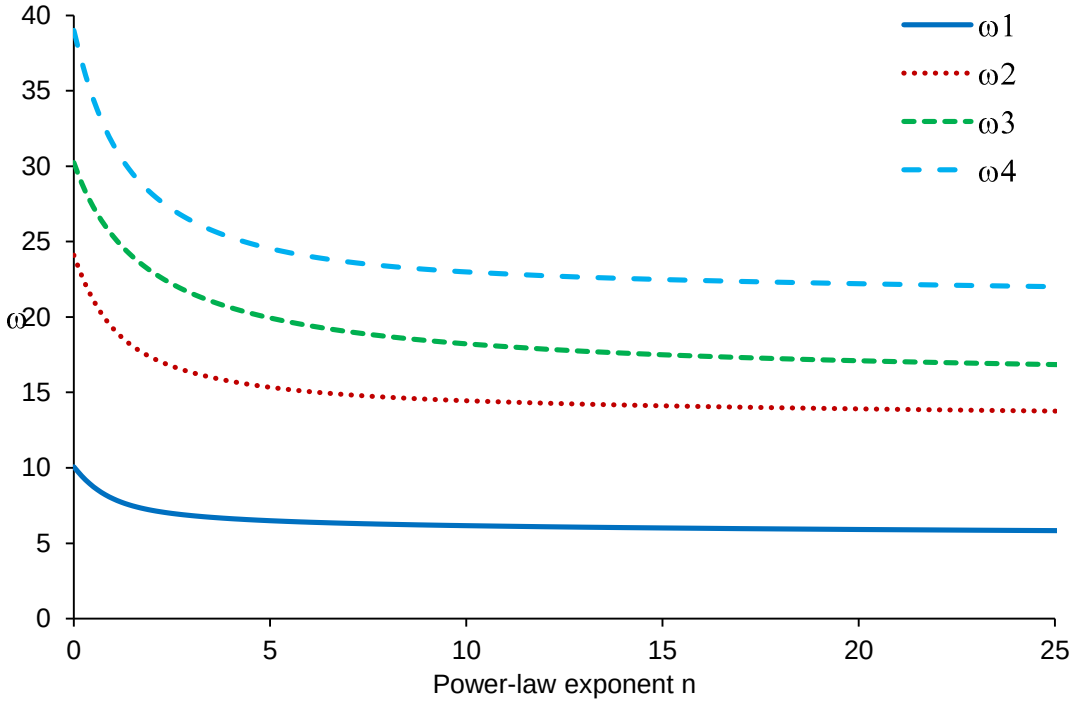

Figure 5: Variation of the first four non-dimensional natural frequenciesof a clamped-clamped FG beamwith respect to power-law exponent (L/h=5).

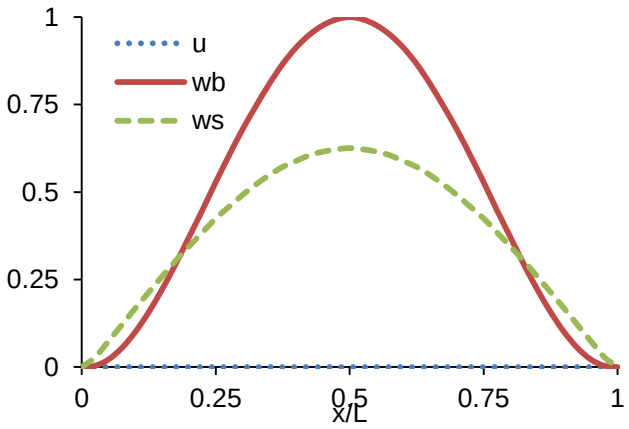

a. Fundamental mode shape ω_1 = 10.0678

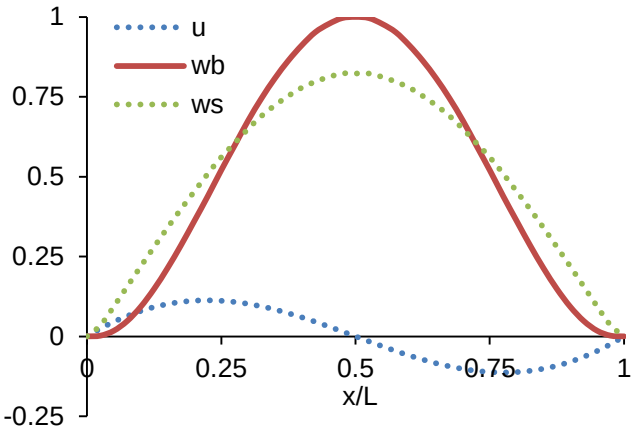

a. Fundamental mode shape ω_1 =6.4961

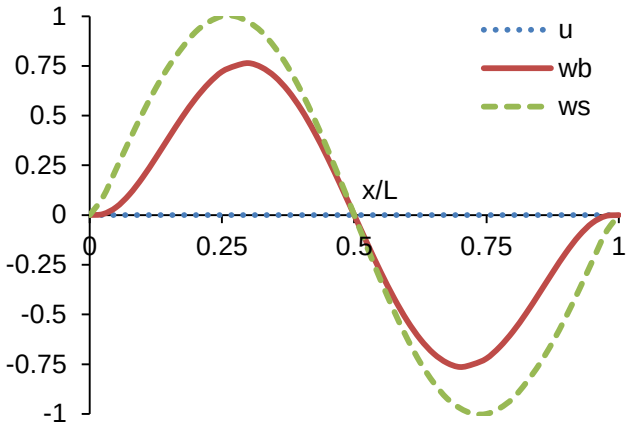

b. Second mode shape ω_2 = 24.1007

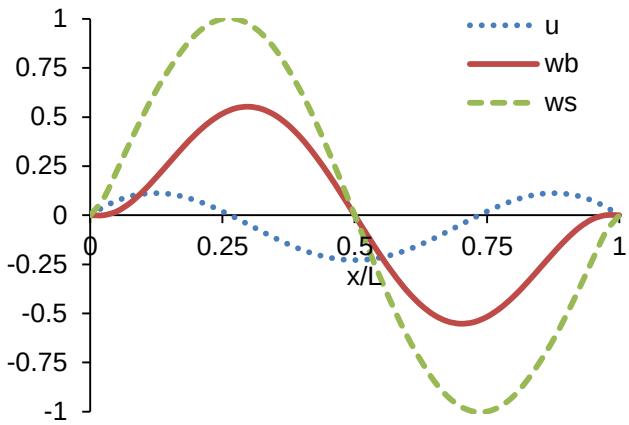

b. Second mode shape ω_2 = 15.3411

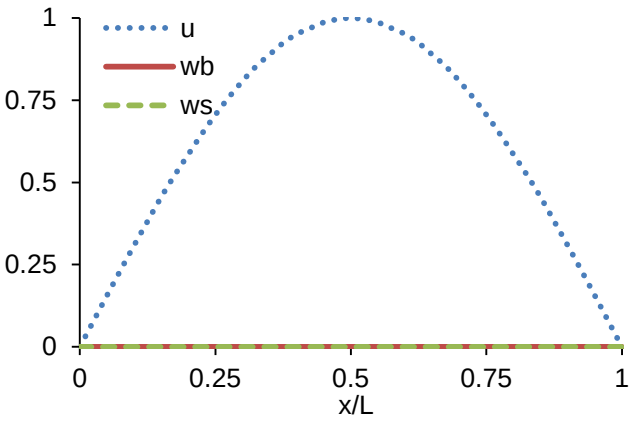

c. Third mode shape ω_3 = 30.2391

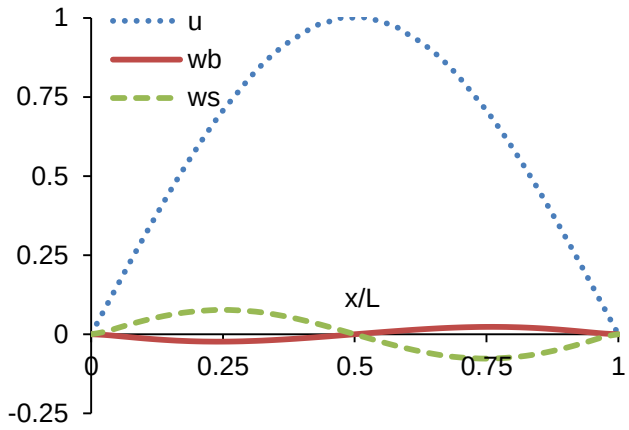

c. Third mode shape ω_3 = 19.9412

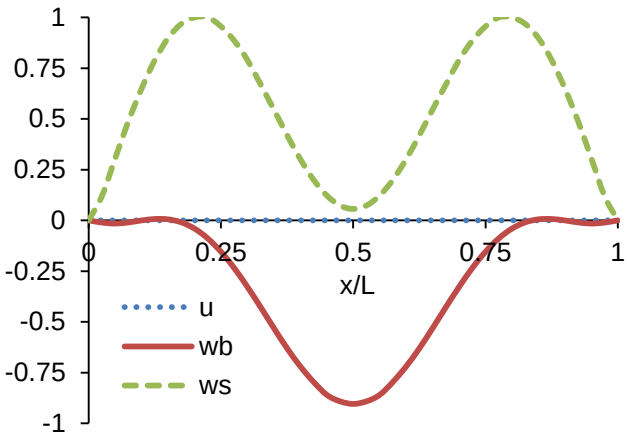

d. Fourth mode shape ω_4 = 39.0057

Homogeneous beam (n=0)

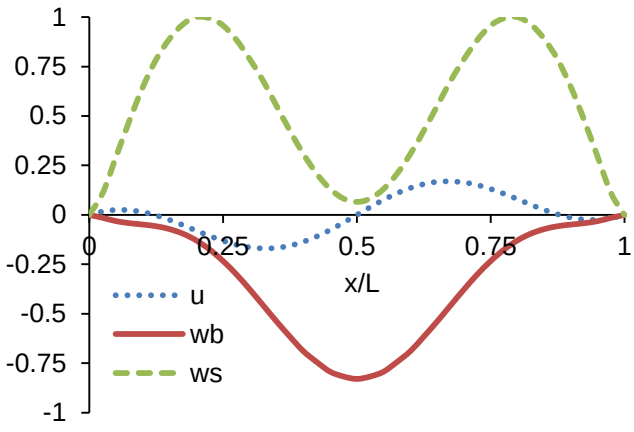

d. Fourth mode shape ω_4 = 24.5432

Functionally graded beam (n=5)

Figure 6: Vibration mode shapes of a clamped-clamped FG beam withtwo values of power-law exponent n=0 and n=5 (L/h=5)

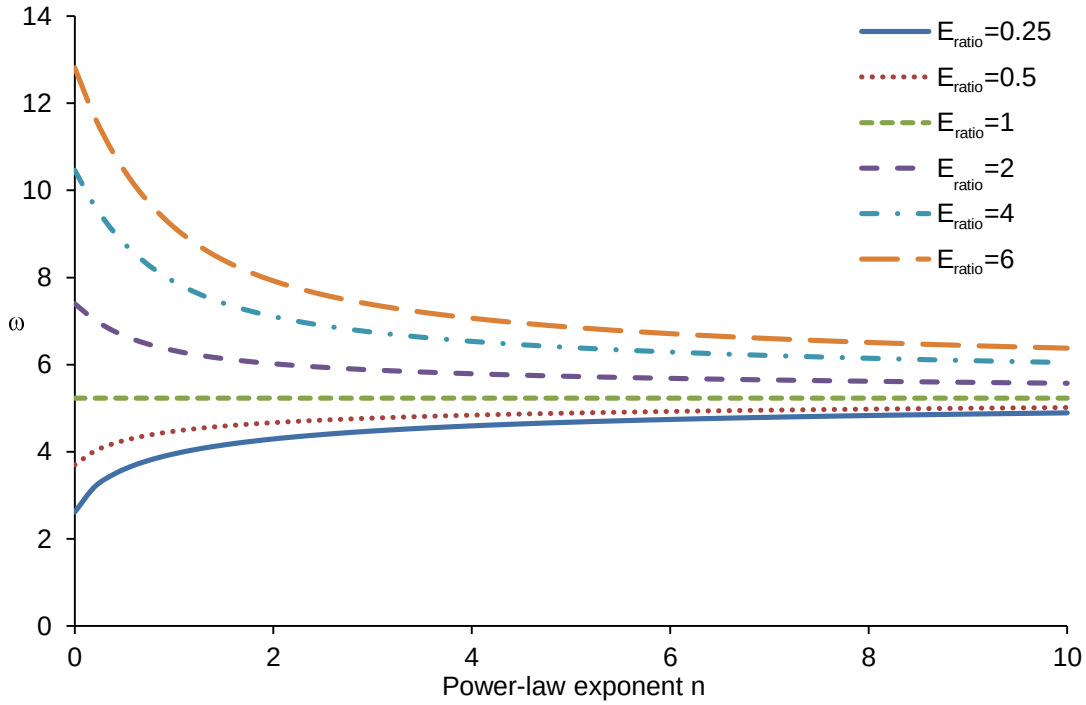

Figure 7: Effect of Young's modulus ratio onthe non-dimensional fundamental natural frequencies of clamped-clamped FG beam with respect to power-law exponent (L/h=5).